

**Cell Reports, Volume 31**

**Supplemental Information**

**Evaluation of Single-Cell Cytokine**

**Secretion and Cell-Cell Interactions**

**with a Hierarchical Loading Microwell Chip**

**Yufu Zhou, Ning Shao, Ricardo Bessa de Castro, Pengchao Zhang, Yuan Ma, Xin Liu, Feizhou Huang, Rong-Fu Wang, and Lidong Qin**

## SUPPLEMENTAL INFORMATION

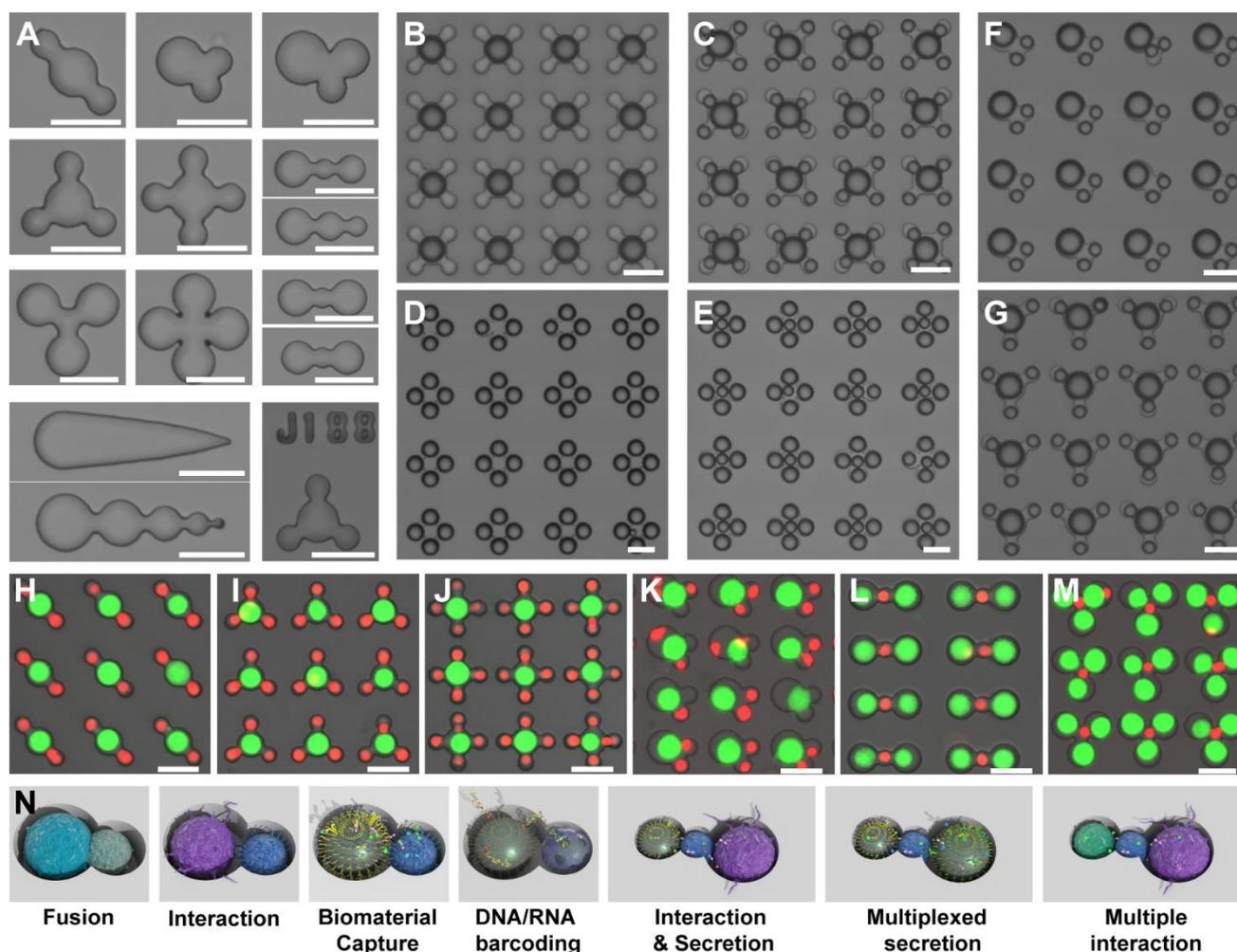


**Figure S1. Customizable bead–bead pairings and cell–cell pairings in HL-Chip.** Related to **Figure 1** and **Figure 2**. (A) Microscopic images of unique shapes possible in the array units. (B)(C) Microscopic images of loading a 4:1 large well-centered array with large beads (B) and small beads (C). (D)(E) Microscopic images of loading a 1:4 small well-centered array with large beads (D) and small beads (E). (F) A microscopic image of a 2:1 small well-clustered array loaded with beads. (G) A microscopic image of a 3:1 large well-centered array loaded with beads. (H) A microscopic image of a 2:1 large well-centered array with cells. (I) A microscopic image of a 3:1 large well-centered array with cells. (J) A microscopic image of a 4:1 large well-centered array with cells. (K) A microscopic image of a 2:1 small well-clustered array with cells. (L) A microscopic image of a 1:2 small well-centered array with cells. (M) A microscopic image of a 1:3 small well-centered array with cells. (N) Schemes of potential applications of HL-Chip. Scale bar, 30  $\mu\text{m}$ .

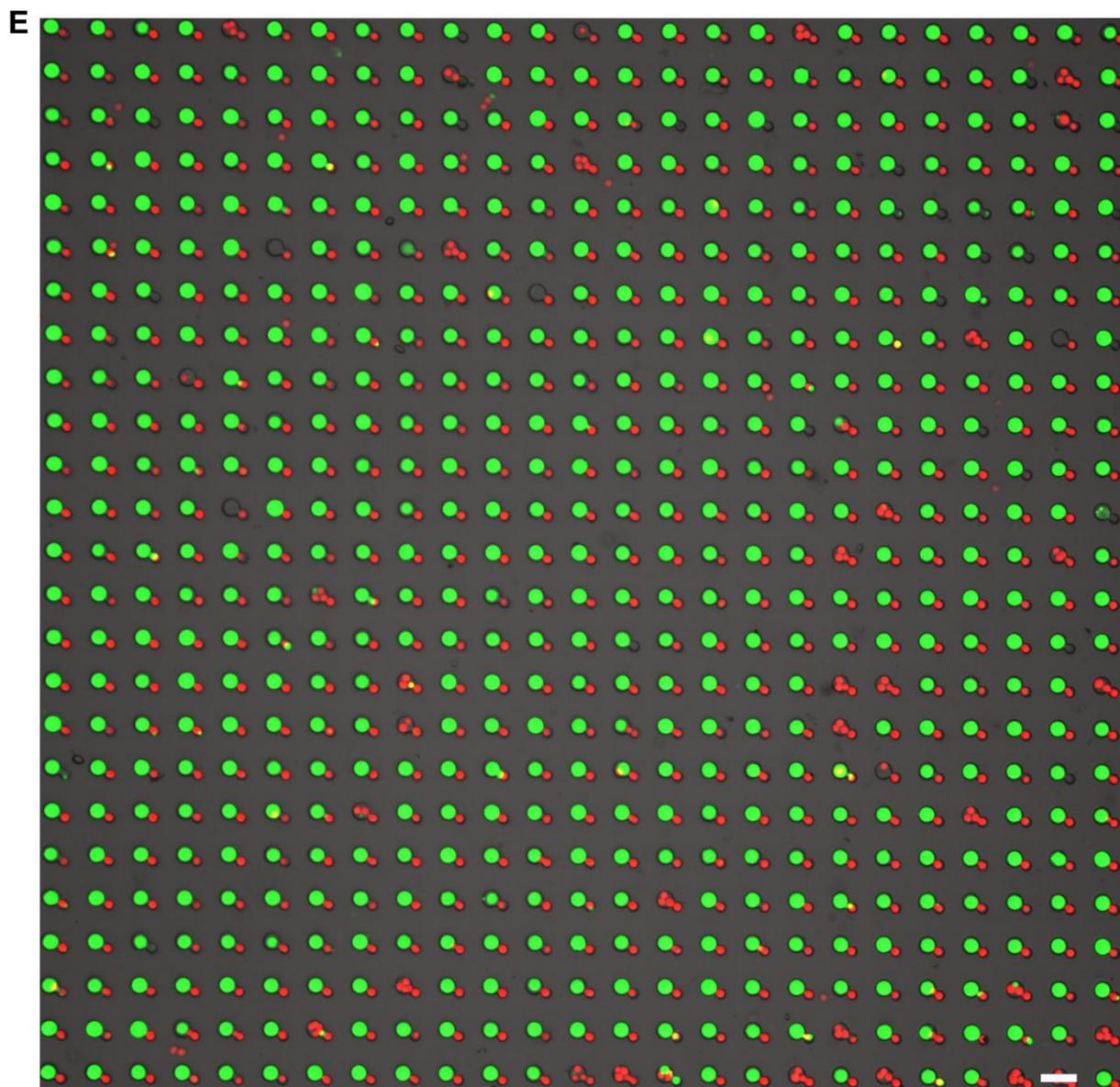
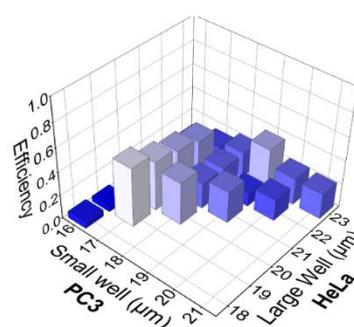
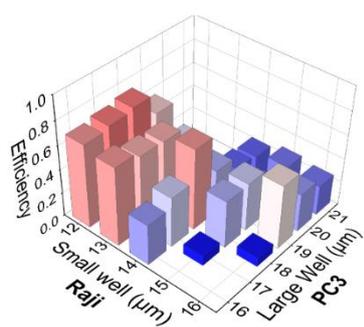
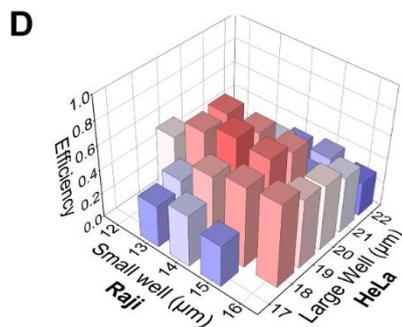
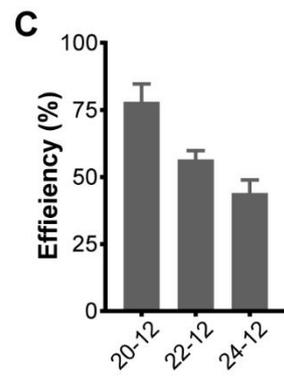
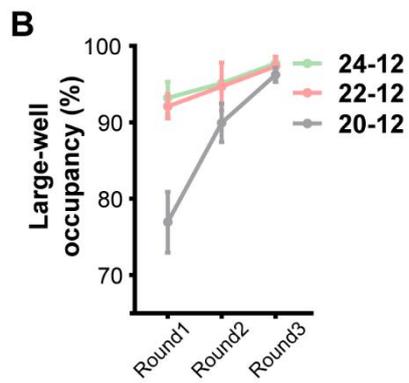
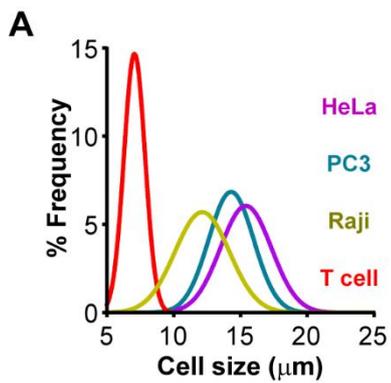


**Figure S2. Optimization for trapping cell–cell pairs in dual-well HL-Chips.** Related to **Figure 2**.

(A) Gaussian distribution fit of the size of T cells, Raji cells, trypsinized PC-3 and HeLa cells. (B) Large-well occupancy of HeLa cells in 20–12  $\mu\text{m}$  (4  $\mu\text{m}$  reduction), 22–12  $\mu\text{m}$  (2  $\mu\text{m}$  reduction) and 24–12  $\mu\text{m}$  HL-Chips by one, two or three rounds of centrifugation. (C) HeLa–T cell pairing efficiency in 20–12  $\mu\text{m}$ , 22–12  $\mu\text{m}$  and 24–12  $\mu\text{m}$  HL-Chips. (D) Pairing efficiency of HeLa–Raji, PC-3–Raji, HeLa–PC-3 in dual-well HL-Chips of different diameters. (E) Overlaid bright field and fluorescent images of HeLa (green)–T cell (red) pairing in a 20–12  $\mu\text{m}$  HL-Chip. Data represent mean  $\pm$  SD from  $n \geq 3$  independent experiments for (B) and (C). Scale bar, 50  $\mu\text{m}$ .

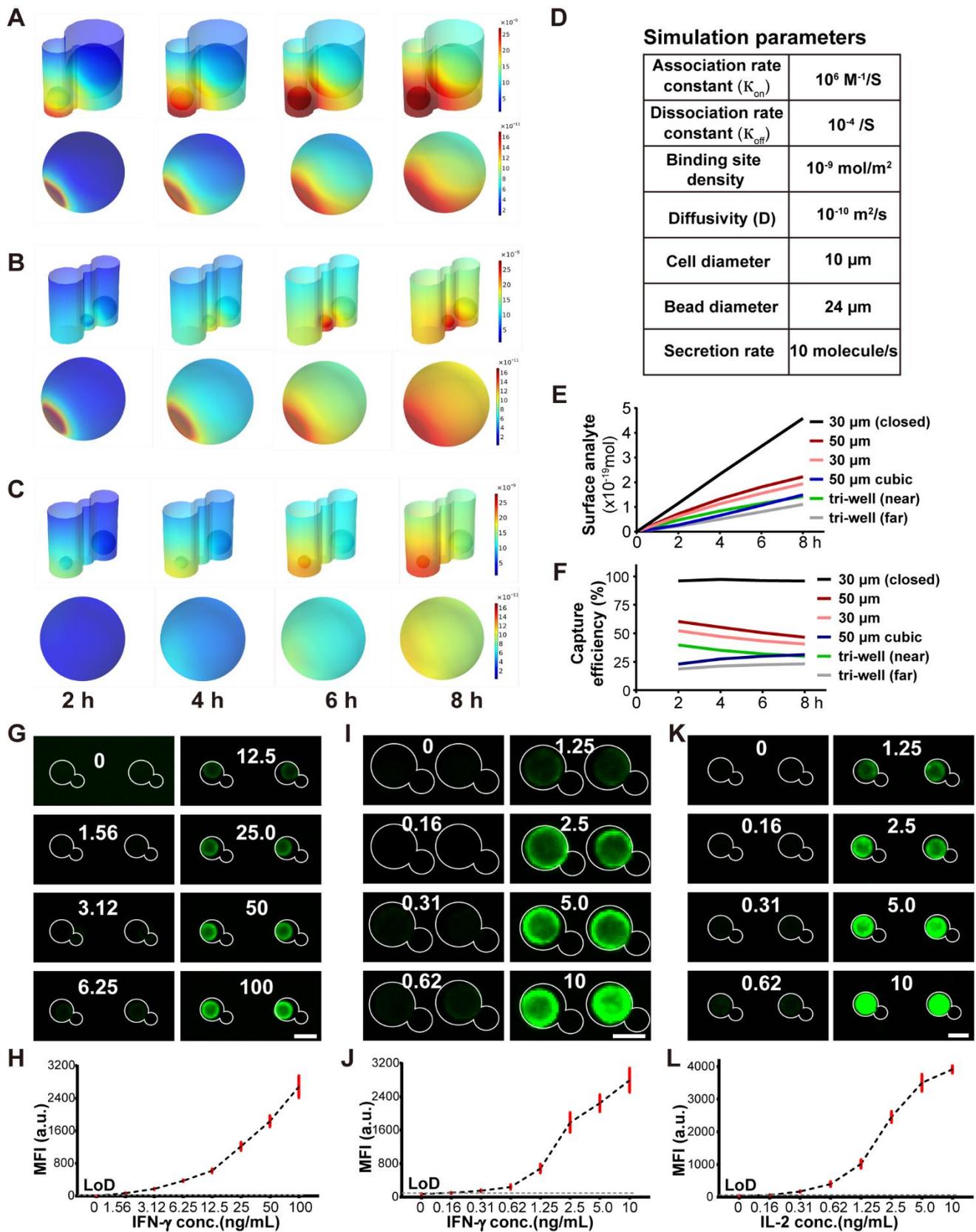


**Figure S3. Finite element analysis to model analyte capture on the bead surface and on-chip calibration using functionalized beads.** Related to Figure 3.

(A)-(C) Sequential heat maps showing the analyte concentration in the bulk medium inside the microwell (upper, unit:

mol/m<sup>3</sup>) and on the bead surface (lower, unit: mol/m<sup>2</sup>) over 2 h intervals. (A) Open 30  $\mu\text{m}$  dual-well configuration. (B) Open 50  $\mu\text{m}$  tri-well configuration where the cell and the bead are near-positioned. (C) Open 50  $\mu\text{m}$  tri-well configuration where the cell and the bead are far-positioned. (D) Simulation parameters adopted in the finite element analysis. (E) Simulated analyte capture on the bead surface in different configurations. (F) Simulated analyte capture efficiency in different configurations. Closed 30  $\mu\text{m}$  dual-well, open 50  $\mu\text{m}$  dual-well, traditional cubic microwells (open, 50x50x50  $\mu\text{m}$ ) were also included in modeling for comparison. (G) Fluorescent images and (H) quantification of background-corrected mean fluorescence intensity (MFI) detected from a minimum of 30 polystyrene beads after on-chip incubation with different concentrations of recombinant human IFN- $\gamma$  using tetrafluorophenyl ester labeled detection antibody. (I) Fluorescent images and (J) quantification of background-corrected MFI detected from a minimum of 30 polystyrene beads after on-chip incubation with different concentrations of recombinant human IFN- $\gamma$  using the TSA detection method. (K) Fluorescent images and (L) quantification of background-corrected MFI detected from a minimum of 30 magnetic beads after on-chip incubation with different concentrations of human IL-2 using the TSA detection method. Data are from one representative experiment of three independent experiments for (G) (I) and (K). Data represent mean  $\pm$  SD for (H) (J) and (L). Scale bar, 20  $\mu\text{m}$ .

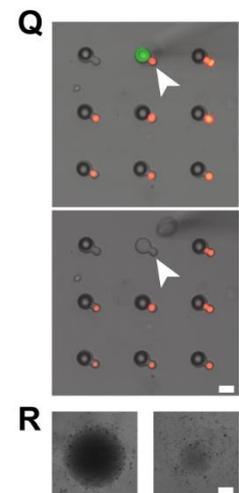
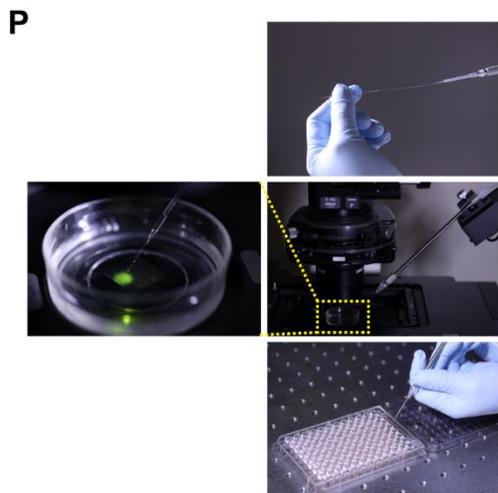
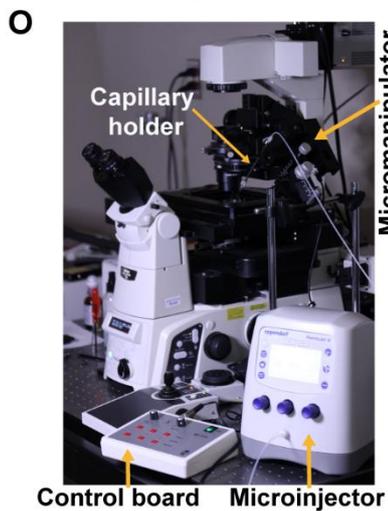
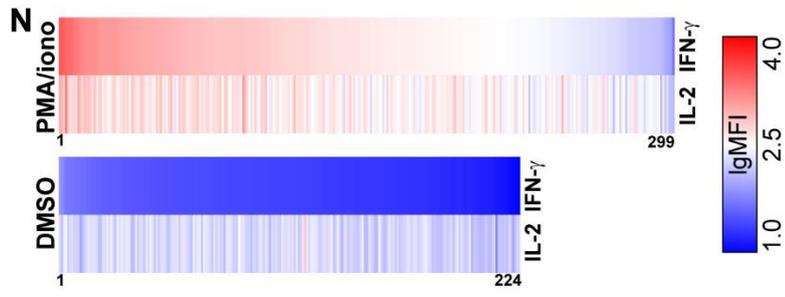
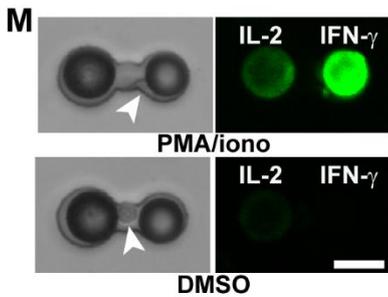
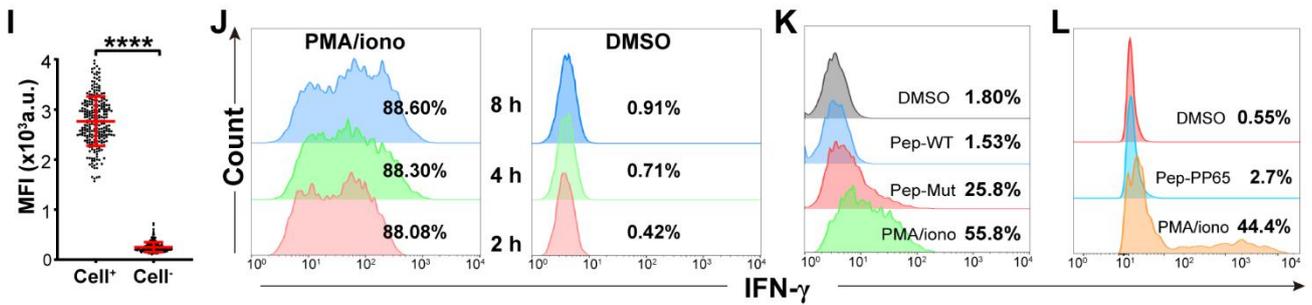
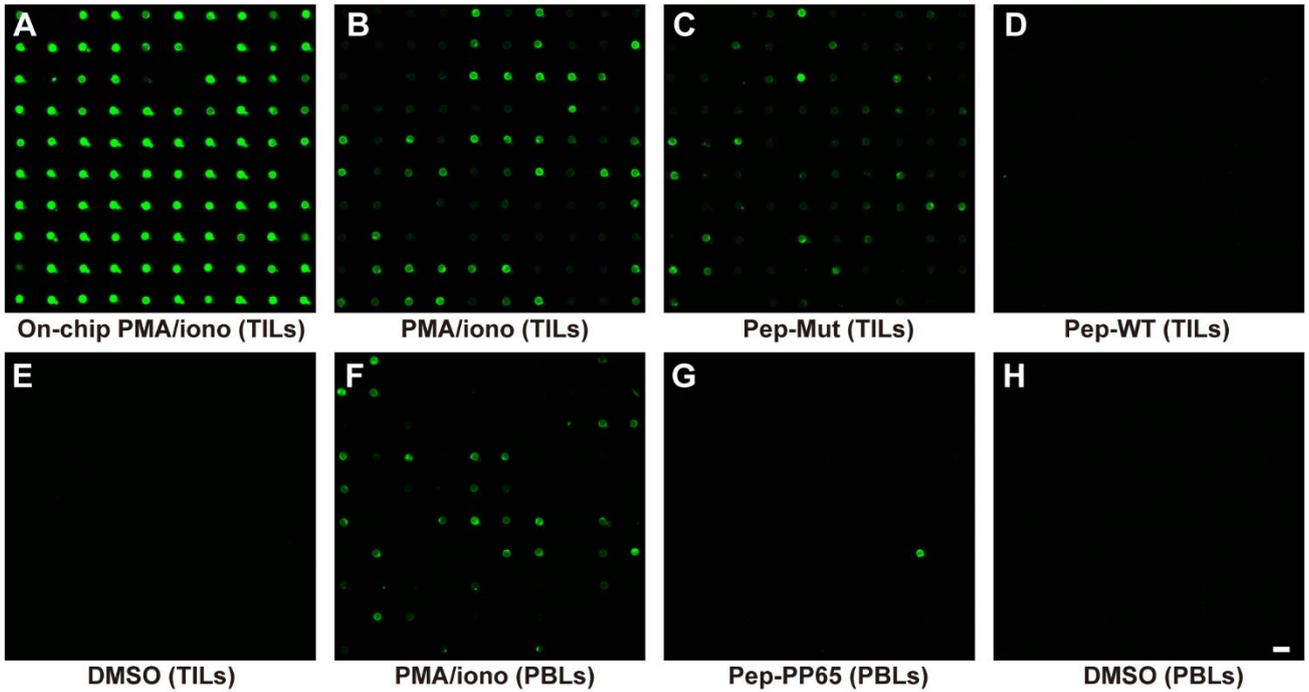


**Figure S4. Characterization of CD-Chip assay. Related to Figure 3.**

(A-H) Microscopic green fluorescent images of beads co-incubating with clonal TILs(2B2) or PBLs using the TSA detection method. TILs were stimulated under following conditions (A-E). (A) Direct on-chip PMA/ionomycin stimulation and incubation for 8 h. (B) On-chip incubation for 8 h after off-chip stimulation with PMA/ionomycin for 8 h. (C) On-chip incubation for 8 h after off-chip pulsing with a mutated peptide specifically recognized by the clone for 8 h. (D) On-chip incubation for 8 h after off-chip pulsing with a wild type peptide for 8 h. (E) On-chip incubation for 8 h after off-chip treated with DMSO as a control for 8 h. PBLs were stimulated under following conditions (F-H). (F) On-chip incubation for 8 h after off-chip stimulation with PMA/ionomycin for 8 h. (G) On-chip incubation for 8 h after off-chip pulsing with PP65 peptide for 8 h. (H) On-chip incubation for 8 h after off-chip treated with DMSO for 8 h. Scale bar for (A-H), 50  $\mu\text{m}$ . (I) MFI of beads from wells co-seeded with cells and adjacent wells without cells after 8 h PMA/ionomycin stimulation. Data represent mean  $\pm$  SD from at least three experiments. (J) ICS staining of the TIL clone 2 h, 4 h, or 8 h after direct stimulation with PMA/ionomycin or DMSO. (K) ICS staining of the TIL clone after stimulation with PMA/ionomycin, the mutated peptide, the wild type peptide or DMSO for 8 h and a subsequent 8 h incubation. (L) ICS staining of PBLs after stimulation with PMA/ionomycin, PP65 peptide or DMSO for 8 h and a subsequent 8 h incubation. (M) Bright field and fluorescent images of concurrent IFN- $\gamma$  (Polystyrene beads, mean size: 18.4  $\mu\text{m}$ ) and IL-2 detection (Magnetic beads, mean size: 21.7  $\mu\text{m}$ ). White arrow heads indicate cell positions. Scale bar, 20  $\mu\text{m}$ . (N) Heatmap for IFN- $\gamma$  secretion is aligned from maximum to minimum with heatmap for IL-2 secretion. Each column represents IFN- $\gamma$  and IL-2 secretion from a single T cell.  $n = 299$  for PMA/ionomycin stimulation and  $n = 224$  for DMSO treatment. Data are from four independent experiments. (O) Device sets for manual cell retrieval. (P) Cell retrieval procedures. Upper, transfer tips were loaded with 5  $\mu\text{L}$  PBS with a micro-loader. Middle, transfer tips were positioned on the top of the well array. Cells paired with fluorescent beads were brought up into transfer tips by reducing compensation pressure. Lower, cells were injected into 96-well plates seeded with irradiated feeder PBLs for clonal expansion. (Q) Microscopic images of the retrieval process. White arrow heads indicate cell positions. Scale bar, 20  $\mu\text{m}$ . (R) A representative image of a retrieved T cell grew into a clone in a 96-well plate seeded with irradiated feeder cells after three weeks (left). The right image depicts a well with only feeder cells. Scale bar, 2 mm.

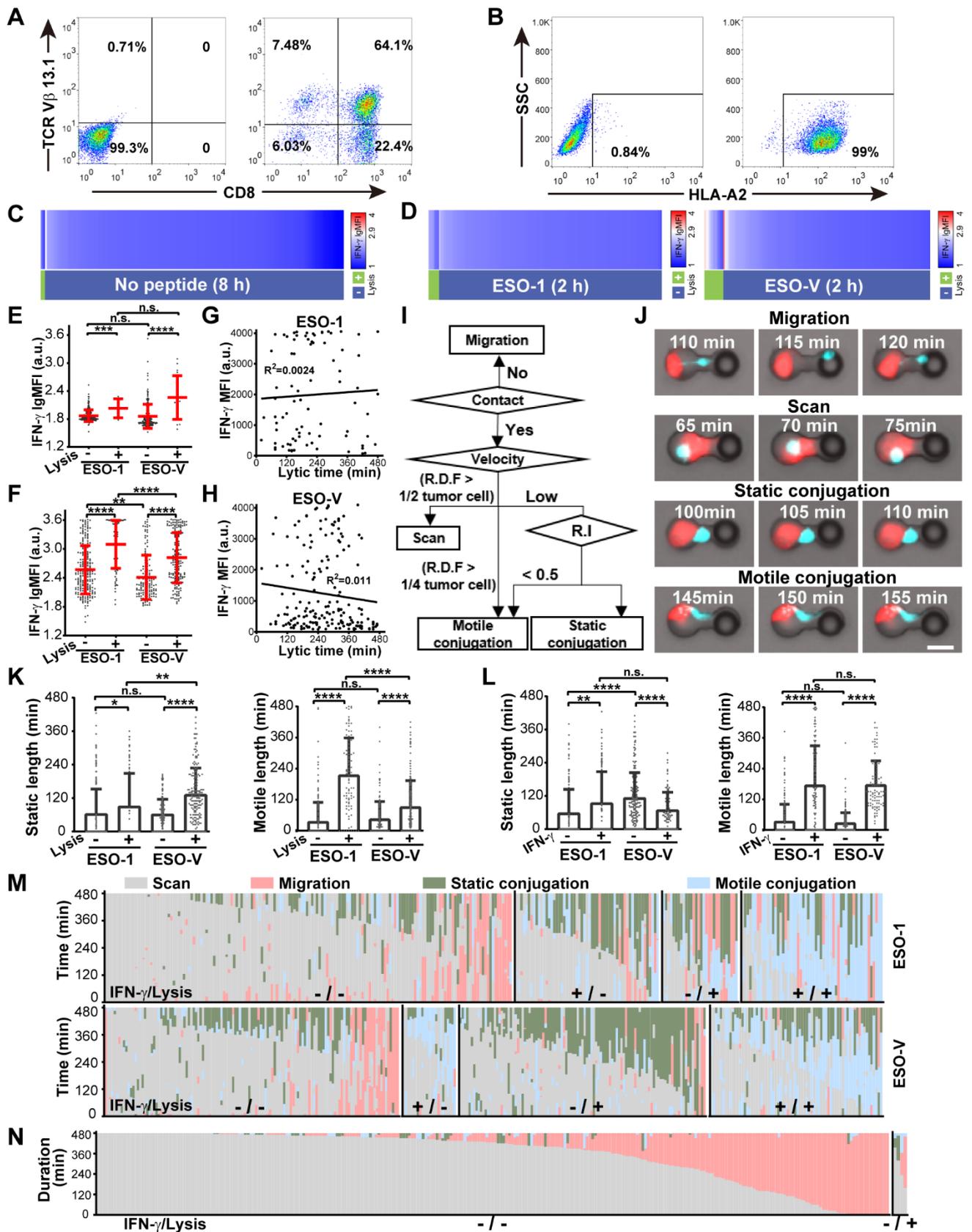


Figure S5. Characterization of NY-ESO-1 T cells interacting with target cells in tri-well HL-Chips. Related to Figure 4 and Figure 5.

(A) Control staining (left) and staining (right) of NY-ESO-1 T cells for transduction efficiency with anti-human TCR V $\beta$

13.1 antibody. (B) Control staining (left) and staining (right) of PC-3/HLA-A2 cells for HLA-A2 expression with anti-human HLA-A2 antibody. (C) Heatmap for IFN- $\gamma$  secretion is aligned from maximum to minimum with cytolytic activity for NY-ESO-1 T cells against target cells ( $n = 289$ ) without pulsing peptide for 8 h. (D) Heatmap for IFN- $\gamma$  secretion is aligned from maximum to minimum with cytolytic activity for NY-ESO-1 T cells against target cells pulsed with NY-ESO-1<sub>157-165</sub> peptide (Left,  $n = 221$ ) or NY-ESO-V<sub>157-165</sub> peptide (Right,  $n = 214$ ) for 2 h. (E) IFN- $\gamma$  secretion in lytic and non-lytic T cells paired with target cells pulsed with indicated peptides for 2 h. (F) IFN- $\gamma$  secretion in lytic and non-lytic T cells paired with target cells pulsed with indicated peptides for 8 h. (G) Correlation of T cells IFN- $\gamma$  secretion with lytic time against NY-ESO-1 ligand. (H) Correlation of T cells IFN- $\gamma$  secretion with lytic time against NY-ESO-V ligand. (I) Defined parameters for classification of NY-ESO-1 T cells interacting with NY-ESO-1(V) peptide pulsed PC-3/HLA-A2 cells in tri-well HL-Chips. Abbreviation: R.D.F., relative displacement per frame. R.I., roundness index. (J) Four classes of interacting phases snapshots. Scale bar, 20  $\mu\text{m}$ . (K) Static and motile conjugation length in lytic and non-lytic T cells paired with target cells pulsed with indicated peptides. (L) Static and motile conjugation length in IFN- $\gamma^-$  and IFN- $\gamma^+$  T cells paired with target cells pulsed with indicated peptides. (M) The exact sequence of phases of NY-ESO-1 TCR-T cells interacting with PC-3/HLA-A2 cells pulsed with NY-ESO-1<sub>157-165</sub> peptide (upper,  $n = 305$ ) or NY-ESO-V<sub>157-165</sub> peptide (lower,  $n = 329$ ). (N) Comparison of phase duration among different functional groups. Each column represents a single target cell–T cell–bead triplet ( $n = 289$ ) with the corresponding phase duration proportionally mapped to the column. LgMFI  $> 2.9$  was defined as IFN- $\gamma^+$ . Data represent mean  $\pm$  SD from  $n \geq 3$  independent experiments for (E) (F) (K) and (L). \*\* $p < 0.01$ , \*\*\* $p < 0.001$ , \*\*\*\* $p < 0.0001$ , by two-tailed Student's  $t$ -test between the indicated groups. Data are from four independent experiments for (C) (D) (M) and (N).

**Table S1. Comparison of cytokine detection methods. Related to Figure 3.**

<b>Method</b>	<b>ICS</b>	<b>ELISPOT</b>	<b>CD-chip</b>
<b>Cytokine forms</b>	Intracellular Membrane retained Secreted	Secreted	Secreted
<b>Resolution</b>	Single cell	Single cell	Single cell
<b>Measurement</b>	Qualitative and quantitative	Qualitative	Qualitative and quantitative
<b>Readout time</b>	6-8 h	24-48 h	2-8 h
<b>Cell number</b>	$> 0.2 \times 10^6$	Vessel limited	$> 1,000$
<b>Cell viability</b>	Lost	Lost	Preserved
<b>Cell retrieval</b>	No	No	Yes
<b>Real-time detection</b>	No	No	Yes
<b>Multiplicity</b>	$N_F$	No	$N_F \times N_B^*$

\*  $N_F$ : the number of fluorophores,  $N_B$ : the number of beads with different sizes.